

Article

Reducing the Erodibility of Sandy Soils Engineered by Cyanobacteria Inoculation: A Laboratory Investigation

Asma Rabiei ¹, Seyed Mohammad Ali Zomorodian ^{1,*} and Brendan C. O'Kelly ^{2,*}¹ Department of Water Engineering, Shiraz University, Shiraz 7144165186, Iran² Department of Civil, Structural, and Environmental Engineering, Trinity College Dublin, D02 PN40 Dublin, Ireland

* Correspondence: mzomorod@shirazu.ac.ir (S.M.A.Z.); bokelly@tcd.ie (B.C.O.)

Abstract: Windblown and water-induced erosion cause substantial soil losses worldwide, especially for drylands. Any sustainable management program that increases soil organic matter and improves the stability of the crustal layer could considerably enhance soil productivity and the preservation of erosion-prone land. This paper presents a laboratory investigation of cyanobacteria-inoculated medium sand and fine sand soils studied for severe runoff conditions that were simulated using an erosion function apparatus (EFA). Loosely deposited sand specimens prepared by air-pluviation were inoculated with a single native filamentous-cyanobacterium strain (investigating both *Nostoc* sp. and *Calothrix* sp.) and then incubated under high exposure to white light for 32- or 48-day periods. Well-developed bio-crusts were produced on the specimens' top surface that achieved substantial improvements in erosion resistance, as was demonstrated for a wide range of hydraulic shear stress investigated using EFA experiments. Relative improvements in hydraulic erosion resistance were explained in terms of the nature of the cyanobacteria-developed microstructures (cyanobacteria filament infiltration of pore-void spaces and exopolysaccharide excretion), as were observed by scanning electron microscope examinations. The developed microstructure depended on the cyanobacterium strain employed and the nominal pore-void sizes that are related to the sand gradation and density state. The encouraging findings of this experimental investigation suggest a tailored approach (i.e., employing a suitable native cyanobacterium strain chosen for its compatibility with the soil's physical properties) could lay the basis for developing a novel technology for soil protection.

Keywords: bio-crust; bio-geotechnics; erosion function apparatus; soil erosion; soil management; soil stabilization; wind erosion



Citation: Rabiei, A.; Zomorodian, S.M.A.; O'Kelly, B.C. Reducing the Erodibility of Sandy Soils Engineered by Cyanobacteria Inoculation: A Laboratory Investigation. *Sustainability* **2023**, *15*, 3811. <https://doi.org/10.3390/su15043811>

Academic Editor: Castorina Silva Vieira

Received: 27 January 2023

Revised: 9 February 2023

Accepted: 14 February 2023

Published: 20 February 2023



Copyright: © 2023 by the authors. Licensee MDPI, Basel, Switzerland. This article is an open access article distributed under the terms and conditions of the Creative Commons Attribution (CC BY) license (<https://creativecommons.org/licenses/by/4.0/>).

1. Introduction

Substantial increases in soil loss rates due to windblown and water-induced erosion are a worldwide issue, especially for drylands, where soils are often fragile and in a vulnerable condition with poor structural stability. The soils' vulnerability depends on moisture, organic matter (OM), and silt contents, along with their texture, cohesive strength, and infiltration capacity. Any sustainable management program that increases OM content and improves soil stability could considerably enhance soil productivity and the preservation of erosion-prone dryland regions that cover approx. 40% of the Earth's surface [1]. For instance, at least 60% of Iran's landmass (being located in semi-arid and arid regions) has been transformed to drylands. Destructive actions, including overgrazing, shrub burning, and over tillage, are causing considerable harm to Iran's soil resources [2]. Emadodin and Bork [3] highlighted population dynamics, deforestation, and overgrazing as the main causes and salinization, alkalinization, waterlogging, soil erosion, and desertification as the main effects of human-induced soil degradation. For instance, from the 1950s to 2008, nearly 5 million hectares of forest in Iran were converted to farmland and urban areas [3]. In

a case study in the north of Iran, Bahrami et al. [4] reported that deforestation and intensive agricultural activities with long-term inappropriate management had caused significant soil degradation. With an estimated rainfall-induced soil erosion rate of ~24 t/ha/year (i.e., fourfold greater than the world average), Iran loses approx. 4 billion tons of soil resource annually [5]. These realities point to the necessity for suitable management practices concerning agricultural development, natural resources, and environment programs [6]. A selection of land management strategies can expectantly reduce soil erosion rates significantly [7]. For instance, mulch addition has been found to be effective in reducing soil losses; straw mulch is easy to apply, contributes soil OM, and is efficient from the day of application [8]. Other environmentally benign approaches and soil additives have yielded some promising results in engineering an improvement in the erosion resistance of treated coarse-grained soils, including, for instance, using bio-cementation via microbial-induced carbonate precipitation (MICP) [9–11] or various biopolymer additives [12–14]. The focus of the present paper is on the development of cyanobacteria-induced bio-crusts (BCs).

Natural BCs, formed as communities of living organisms on the soil surface in the open spaces of drylands, shield about 12.2% of the Earth's surface [15,16] and play vital roles in the establishment, growth, and bio-fertilizing of vascular plants, as well as having essential influences on soil formation, protection, and bioremediation [17,18]. Microorganisms (e.g., bacteria, cyanobacteria, lichens, and some microscopic green algae) form the vast portion of dryland BCs [19], with, for instance, around 320 cyanobacteria species accurately identified [20]. As worldwide bio-resources, cyanobacteria have unique abilities for improving soil stability by stimulating biological activity, producing OM and exopolysaccharide (EPS) substances that enmesh the soil particles/aggregates [21–24]. Filamentous cyanobacteria (e.g., *Microcoleus vaginatus*, *Scytonema*, *Schizothrix*, *Calothrix*, *Chroococcidiopsis*, *Nostoc* and *Phorimidium*) represent the most primitive microorganisms in the BC mats of the topsoil layer [25]. They produce EPS substances as protective sheaths [26], which preferentially bind the soil particles via gluey, interwoven, and entangled filaments, resulting in BC development [24,27,28]. These microorganisms have special adaptation skills in severe climatic and edaphic circumstances [17,22]. For instance, with their chlorophylls and other pigments, such as *Phycocyanins* and *Phycocerytrins*, cyanobacteria are capable of protecting themselves against intensive solar radiation and harmful ultraviolet rays [29]. As their sheaths or capsules form, the emitted EPS can hold water and thereby, the cyanobacteria tolerate arid climate. Species such as *Scytonema hyalinum*, *Scytonema crispum*, *Nostoc commune*, *Nostoc* sp. and *Calothrix parietina* can survive extreme heat and desiccation [17]. These species form bundles of filaments enclosed by gelatinous sheaths; the intermingled filament bundles create a three-dimensional (3D) net-like structure within the soil pore voids that binds neighbouring soil particles with the potential to stabilize the surficial soil layer in a crust.

Whereas previous research on cyanobacteria inoculation has mostly focused on increasing crop yields, the last decade has seen increased emphasis on investigating cyanobacteria inoculation as promising a cost-effective and eco-friendly biological solution for achieving improvements in soil quality and reduced erosion rates for vulnerable sandy soils [21,22,24,26,30–32]. Most of these studies, e.g., [30,33–38], investigated biologically-treated windblown agricultural soils that initially had moderate–high nutrient conditions. Severe runoff conditions in biologically treated low-nutrient soils, as investigated in the present paper, is identified as a knowledge gap. These studies also employed a mixture of cyanobacteria microorganisms or strains for biological treatment. Cyanobacteria-developed microstructures differ depending on the soil's physical properties and the cyanobacteria's morphological characteristics [39].

An interesting hypothesis, therefore, concerns tailoring the cyanobacteria-developed soil improvement approach to the particular soil type undergoing treatment by employing a single cyanobacterium strain chosen for its compatibility with the soil physical properties (principally gradation and density state). This approach could lay the basis for developing a technology for soil protection based on cyanobacteria inoculation.

Recently, the authors [24] reported on the efficacy of cyanobacteria inoculation for medium–coarse silica sand. The present experimental laboratory investigation sets out to examine two loosely deposited silica sands with different grading (i.e., fine sand (FS) and medium sand (MS) soils) in a severe runoff simulation using an erosion-function apparatus (EFA). These sands, especially FS, are more prone to erosion because of their smaller grain sizes, being categorized as having high/very high erodibility potential. Focusing on the problem of land degradation in the drylands of Iran, two native cyanobacteria strains, *Nostoc* sp. and *Calothrix* sp., were chosen for this investigation because of their abundant existence in soil environs, rapid growth phase and tolerance of harsh environmental conditions, and their filamentous morphology and high EPS excretion ability for BC formation. Therefore, the aims of the present laboratory investigation are:

- To examine the efficacy of cyanobacteria inoculation by using single native cyanobacteria strains of *Nostoc* sp. or *Calothrix* sp. for reducing the erodibility of loosely deposited fine and medium gradation sands tested under severe runoff conditions.
- Establish the nature of the cyanobacteria-developed microstructures for the different gradation sands.
- Explain the relative improvements in hydraulic erosion resistance in terms of the nature of cyanobacteria-developed microstructures formed depending on sand type (gradation) and cyanobacterium strain employed.

2. Experimental

2.1. Materials

2.1.1. Sand Source and Physical Characteristics

Clean MS and FS soils, as classified according to the Unified Soil Classification System (USCS) [40], were examined in the present investigation because of their high/very high erodibility potential. The test soils were obtained from the Chirook sand mine near Chirook village, Deyhuk Rural District, Tabas, Iran. This site was chosen for convenience and had been previously used by the authors as a sand source for bench-scale investigations of other soil improvement options. These included the bio-cementation of a loose medium-sand crustal layer using the MICP technique applied by spray treatment for mitigating wind erosion [11], MICP treatment of dense medium sand specimens by various reagent-injection strategies [10], stabilizing dense medium sand with 1–4 wt% nano-silica additive [41], and cyanobacteria inoculation of medium–coarse sand [24] for improving hydraulic erosion resistance.

Both test sands in the present investigation were comprised of sub-angular grains. With D_{10} , D_{30} and D_{60} (i.e., the sand particle sizes corresponding to 10, 30, and 60 wt% passing) of 0.14, 0.19, and 0.26 mm, respectively, the FS material had coefficients of uniformity $C_U (=D_{60}/D_{10})$ and curvature $C_C (=D_{30}^2/D_{60} D_{10})$ values of 1.9 and 1.0, respectively. Similarly, with D_{10} , D_{30} and D_{60} of 0.36, 0.63, and 0.83 mm, respectively, the MS material had C_U and C_C values of 2.3 and 1.3, respectively. The mean particle sizes (D_{50}) of FS and MS were 0.23 and 0.77 mm, respectively, and each sand had a fines content (i.e., soil particles sized < 0.075 mm) of approx. 1 wt%. With $C_U < 6$ [40], both sands are classified as poorly graded (SP). Their specific gravity of solids was determined as 2.67.

In advance of the specimen preparation stage (Section 2.2.1), samples of the sand materials were washed to remove fines and then sterilized by oven drying at 105 °C for 48 h [39]. After turning the oven off, the samples were allowed to cool overnight (by a slight opening of the oven door) to attain an ambient laboratory temperature of between 25 and 28 °C. The following morning, the cooled sterilized sand materials were placed in hygienic plastic containers.

2.1.2. Cyanobacterial Solution Formation

Pure *Nostoc* sp. and *Calothrix* sp. cyanobacteria stocks were sourced from the algal collection of Shahid Beheshti University. The isolated strains, extracted from the paddy fields of Khuzestan (Iran), can be cultivated in a growth medium lacking chemical compounds of

nitrogen because of the unique skill of the heterocyst cells in fixing atmosphere nitrogen. For this investigation, BG-11₀ culture medium [42] was prepared using filter sterilization and then stored in sterile containers at 4 °C. The desired amount of BG-11₀ medium was autoclaved at 138 kPa pressure and 120 °C temperature for 45 min in Erlenmeyer flasks at pH 7. Two sterilized culture mediums were separately inoculated using *Nostoc* sp. and *Calothrix* sp. pure stocks and then continuously aerated at a medium rate in sealed glass flasks under controlled environmental conditions. Cool white light-emitting diodes (LEDs) positioned 80-cm above provided 70 $\mu\text{mol photons/m}^2/\text{s}$ intensity in an isolated room maintained at 30 ± 2 °C. Daily use of a sterile stirrer up to the middle of the exponential growth phase caused a delicate detachment of the growing cyanobacteria from the inner wall of the glass flasks. A fresh biomass weighing approx. 16.6 mg/mL of inoculum medium (equating to 0.33 mg/mL of dry matter for freeze-dried material) was produced using an MPW-351R centrifuge operating at 10,000 rpm for 15 min.

2.2. Experimental Program

2.2.1. Preparation of Sand Specimens

Each sand test-specimen was prepared by air-pluviation that loosely deposited the dry, sterile material into a transparent plastic container of 6.5-cm internal diameter and 5.6 cm deep. Each sterilized container was fitted at its base with a mesh fabric filter and a bottom drainage tube. The dry sand was allowed to free-fall from an elevation of 20 cm by opening the valve of a miniature sand-raining device (see Figure 1) in order to deposit a 5.5-cm deep layer in each specimen container (i.e., almost completely filling them with sand). For FS and MS, the deposited specimens had void ratio values of 0.57 and 0.49, respectively, with corresponding dry densities of 1.69 and 1.78 Mg/m^3 . For both sands, the water holding capacity (i.e., volume of pore-void spaces, V_v) of each test specimen was approx. 60 mL.

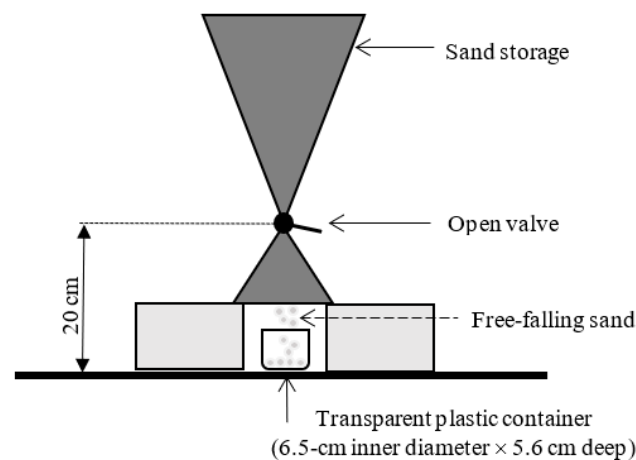


Figure 1. Schematic sketch of the set up used to prepare loose, uniform sand test-specimens by the air-pluviation method.

2.2.2. Specimen Inoculation and Incubation Procedures

The cultured cyanobacteria mediums were used to inoculate the prepared sand test-specimens as follows. With an extension collar provided by plastic film wrapped around (and sealed on) the containers' outer top rim and the bottom drainage tube fully open, 120 mL of distilled water (i.e., $\sim 2 \times V_v$) was carefully poured onto the top surface of each sand specimen. The ponded water slowly percolated down through the test specimen, and once 60 mL of the water had drained away via the bottom drainage tube (i.e., so the specimen's full water holding capacity was achieved), the drainage tube was closed permanently. In this way, the air contained in the pore-void spaces was purged from the specimen [10]. Next, for each test-specimen undergoing treatment, 30 mL of homogeneous cyanobacterial inoculum was carefully poured onto the top surface to provide 0.5 g of fresh cyanobacteria biomass. For each non-inoculated sand specimen, 30 mL of distilled

water was used instead. All test specimens were incubated under the same constant environmental conditions. They were placed in sterile water baths maintained at 30 ± 2 °C and continuously illuminated with white 5000 lx fluorescent lights positioned 80 cm above the specimens' top surface. For the full duration of the incubation periods (i.e., 32- and 48-day periods investigated), all specimens were irrigated daily with the precise injection of 2.5 mL of distilled water.

2.2.3. Investigated Specimen Groups

Three specimen groups were investigated; that is, the *Nostoc*- and *Calothrix*-inoculated groups—abbreviated for specimen labelling purposes as 'N' and 'C', respectively—and the non-inoculated (control) group, abbreviated simply as FS or MS. The level of biological activity for cyanobacteria-inoculated specimens depends on the incubation period, with 32- and 48-day incubation examined in the present study, as previously used in investigations by [24,38,43]. Hence, the two inoculated specimen groups were each subdivided according to 32- or 48-day incubation, differentiated by '32' and '48' appearing in the treated group names.

For biologically treated specimens, a clear gap formed between the BC (developed over the specimens' top surface) and their containers' sidewall during the incubation period: see Figure 2a, which shows the situation developed for an extended 120-day incubation period for clearly illustrating this point. This separation between the formed BC and the container's sidewall occurred because microbial growth was inhibited on the surfaces of the plastic containers on account of their impermeability. For these bench-scale experiments, an assessment of the formed BC as a continuous protective surficial layer (to resist hydraulic shear) was investigated by bonding the BC to the container sidewall (see Figure 2b), which was done one hour before the start of the EFA testing. On the other hand, EFA testing of the unattached BC group provided an opportunity to evaluate the BC's entanglement to the underlying sand layer. In naming these treated test-specimens, the BC edge condition was differentiated by 'A' and 'D', denoting attached and detached BCs, respectively. For instance, N/48/A refers to a 48-day incubated, *Nostoc*-inoculated specimen with BC attached to the container sidewall. Three replicates were tested for each investigated scenario, with the EFA testing program examining 336 inoculated and 42 non-inoculated test-specimens.



Figure 2. (a) Detached BC and (b) attached BC (herein identified as specimen groups with 'D' and 'A', abbreviations, respectively).

2.2.4. Microstructure Assessment of Treated Sand Specimens

To observe the structural characteristics of the sand grain connections formed with the cyanobacterial filaments and EPS, dried BCs of the treated sand specimens were cropped and then coated by gold sputtering to prepare samples for imaging analysis at different magnifications using TESCAN-vega3 scanning electron microscope (SEM) equipment operated in high-vacuum mode (20 kV).

2.2.5. EFA Testing Program and Calculations

Based on the principles of the EFA device developed by Briaud et al. [44], Shiraz University's purpose-built recirculating EFA employed in the present investigation has a 2.0-m long conduit with internal cross-sectional dimensions of 12 cm wide by 6 cm high (Figure 3a,b). A 6.5-cm dia. hole, located 1.3 m along the conduit's length (measured from its entrance) and centered on its base dimension (see Figure 3a), provides secure placement for one of the sand containers. Before the start of each EFA test, the top surface of the test specimen was aligned flush with the conduit's inner bottom wall. A valve at the conduit inlet (Figure 3c) redirects the water flow and provides adjustment of the flow rate. Beyond the conduit outflow, a point gauge of 0.1-mm accuracy and triangular weir arrangement positioned near the end of a channel (Figure 3e) allows measurement of the flow rate. The upper-bound flow discharge investigated was restricted by the maximum channel capacity, while the lower-bound flow investigated was determined by the critical flow velocity of the non-inoculated sand specimens.

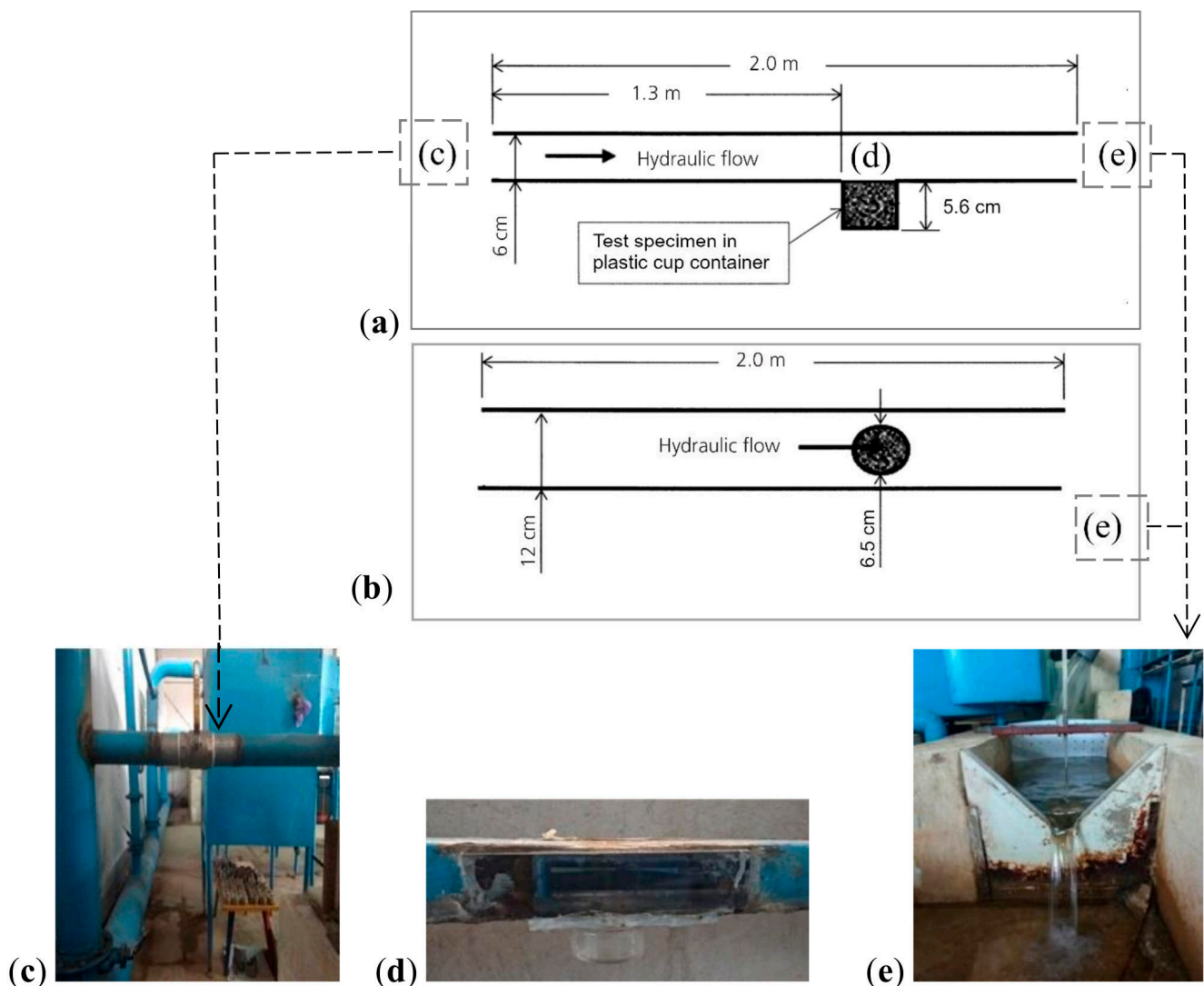


Figure 3. University of Shiraz EFA: (a) longitudinal cross-section and (b) plan view schematics of 2-m long recirculating conduit; (c) inlet valve placement near conduit entrance; (d) Plexiglas side window for observing exposed top surface of the test-specimen held in plastic container fitted to the underside of the conduit; (e) triangular weir and point gauge flow-measurement system (adopted from Rabiei et al. [24]).

After regulating the flow discharge to achieve the required mean flow velocity, the inlet valve was opened, thereby redirecting the flow to occur along the conduit. A transparent Plexiglas window in the conduit sidewall (Figure 3d) allowed observation of the specimen erosion rate as the EFA test progressed. The interval time (Δt) from the opening of this valve and achieving a homogeneous sand erosion was measured using a chronometer. Once achieved, the inlet valve was closed, redirecting the flow away from the conduit, with any water remaining within the conduit allowed to drain away towards the channel end. The specimen container was then carefully removed from the underside of the conduit. The eroded sand volume (V_e) from the test specimen, determined as the amount of water needed to completely fill the erosion scour, was measured using a graduated syringe. The mean erosion depth was calculated as $d_e = V_e / A_s$, where A_s is the specimen's cross-sectional area (constant for all test-specimens), with the erosion rate calculated as $E = d_e / \Delta t$.

The testing program investigated mean flow velocity (V) values, in ascending order, of 0.43, 0.56, 0.72, 0.80, 0.90, 1.0, and 1.1 m/s. Common types of erosion-function charts plot the erosion rate against V or the hydraulic shear stress (τ), both of these approaches being employed later in this paper for presenting the experimental results.

Note, for V [m/s], the τ magnitude [Pa] acting at the sand–water interface can be computed as

$$\tau = \frac{1}{8} \rho_w f V^2 \quad (1)$$

where ρ_w is the density of water [kg/m^3], and f is the friction factor obtained from the Moody chart [45], which relates f to the Reynold's number (Re) and relative roughness (ϵ') parameters, these being estimated as follows

$$Re = \frac{VD}{\nu} \quad (2)$$

$$\epsilon' = \frac{0.5 D_{50}}{D} \quad (3)$$

where ν is the kinematic viscosity of the fluid (water) at 20 °C, D is the hydraulic diameter of the rectangular cross-sectional conduit, and D_{50} is the mean particle size (of the sand materials tested).

Erosion resistance can be quantified using the erosion coefficients (K_V and K_τ) and erodibility thresholds (V_c and τ_c). The most erodible soils have values of $V_c < 0.5$ m/s and/or $\tau_c < 1$ Pa [46]. K_V and K_τ were obtained as the gradients of the best-fit linear regression lines in the plotted E – V and E – τ erosion function charts, respectively. Here V_c and τ_c were calculated by modifying the Shafii et al. method [47]—that is, their magnitudes were determined as the intersection point with the horizontal axis (V or τ) of the extrapolated line joining the first two ascending data points on the erosion curve in the bi-logarithmic plot, with the lowest erosion rate assumed as 100 mm/h.

3. Results and Analysis

3.1. Visual Appearance of Treated Specimens and SEM Observations

Figure 4 shows the top and side views of randomly selected cyanobacteria-inoculated and non-inoculated specimens for both sand types with a 48-day incubation. Homogeneous BC formation, with crust thickness of approx. 1 mm, uniformly covered the top surfaces of all inoculated specimens. On close examination, the *Nostoc* and *Calothrix* filaments were observed to infiltrate successfully in the depth of the treated MS, but this was not traceable for treated FS specimens.

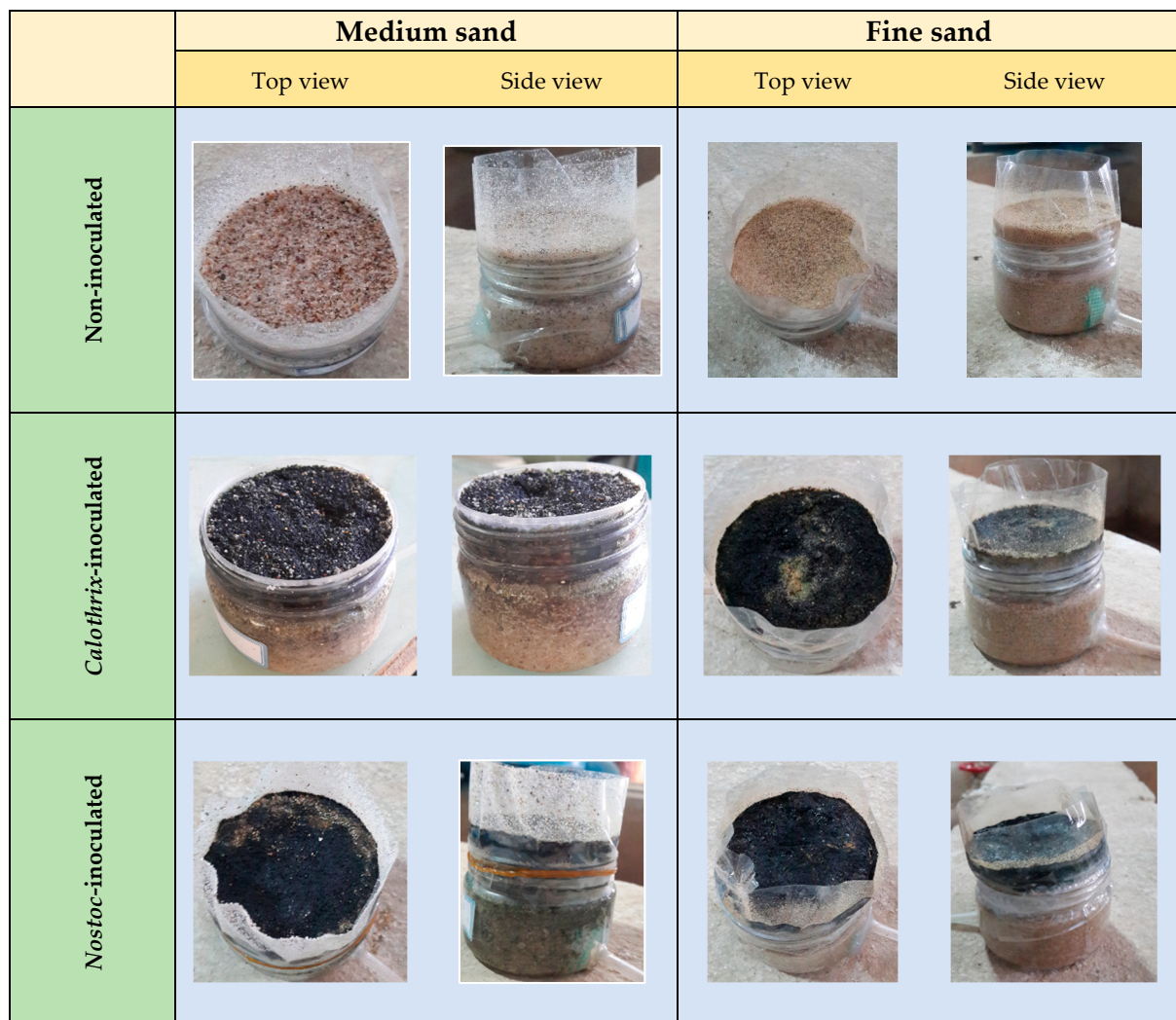


Figure 4. Non-inoculated and cyanobacteria-inoculated specimens with a 48-day incubation. Note the extension collars of plastic film wrapped around (and sealed using elastic bands on) the plastic containers' outer top rim.

Figure 5 shows various SEM images of non-inoculated and *Nostoc*- and *Calothrix*-inoculated FS. Figure 5a,b illustrate its sub-angular grains and, compared to MS, its smaller pore-void spaces between grains. Figure 5c,d show the *Calothrix* filament-entangled FS grains, with the filaments infiltrated properly in the narrow gaps between neighboring grains, and the structured intertwined network of the aggregated fine grains and *Calothrix* filaments. Figure 5e,f show a non-uniform network of *Nostoc* strain around FS grains—that is, the *Nostoc*-excreted EPS acted as coverage on the grains but, compared to the *Calothrix*, it had less homogeneity in the pore void spaces. This contrasted with observations for MS, and also a medium-coarse gradation sand previously investigated by the authors [24], where the excretion of EPS in the *Nostoc* inoculated sand produced uniform blanket coverage of the grains binding them together. In other words, these observations indicate different binding emphases depending on the sand gradation and cyanobacterium strain employed.

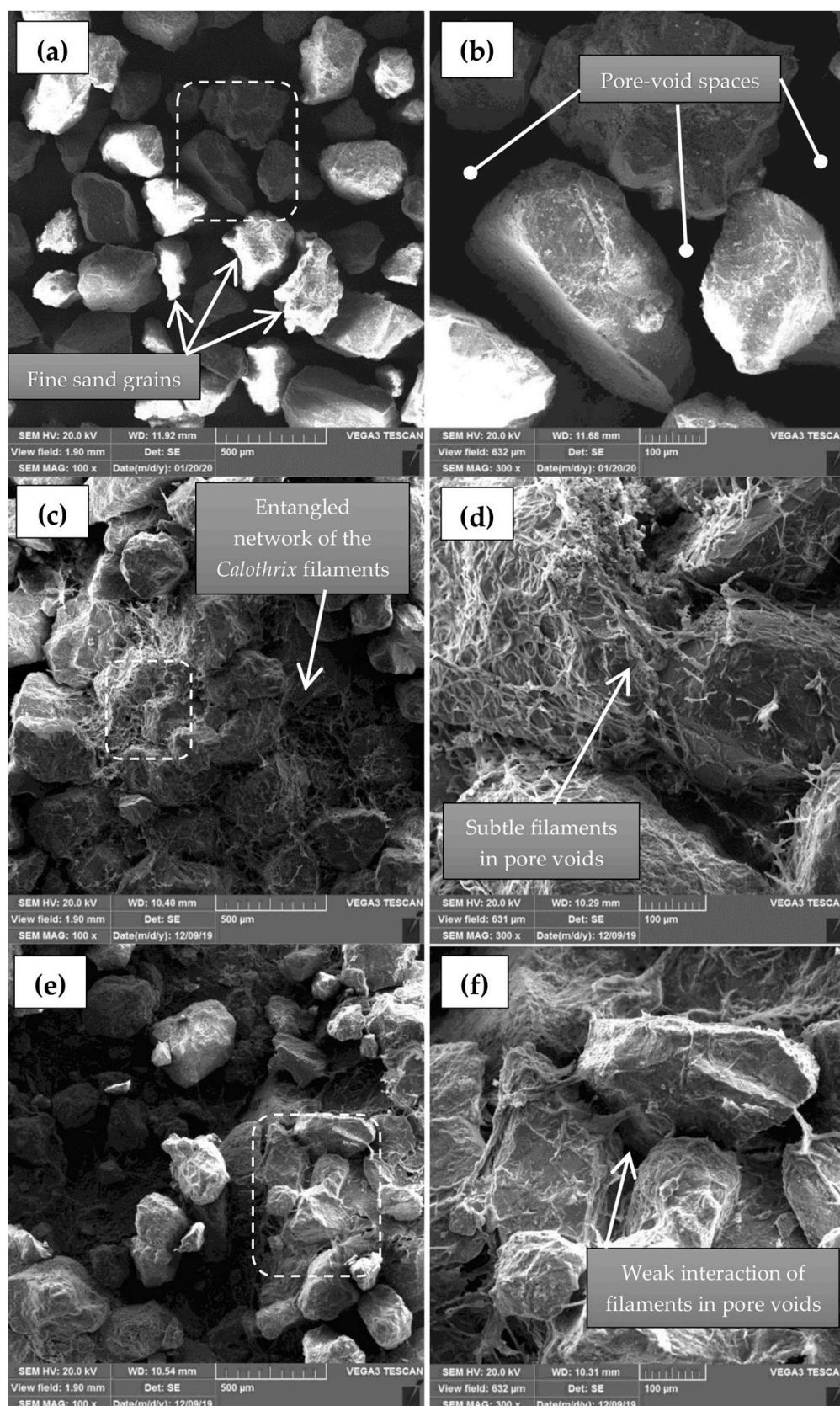


Figure 5. SEM images of: (a,b) non-inoculated; (c,d) *Calothrix* treated; and (e,f) *Nostoc*-treated fine sand taken at 100× and for 300× magnifications focusing on the dashed rectangular areas.

3.2. EFA Test Results

Figure 6 presents the E - V and E - τ erosion-function charts for the two cyanobacteria-treated sand types, and also includes data for the non-inoculated (control) specimens, all of which were EFA tested with detached BC. Figure 7 presents the E - V and E - τ plots for those specimens tested with their BC attached to the container sidewall. Figures 8 and 9 present a series of plots for those specimens tested with detached BC illustrating the interdependence for the loose MS and FS soils of (i) cyanobacterium strain and flow velocity on erosion rate (Figures 8a and 9a), (ii) cyanobacterium strain and incubation period on erosion rate (Figures 8b and 9b), and (iii) incubation period and flow velocity on erosion rate (Figures 8c and 9c).

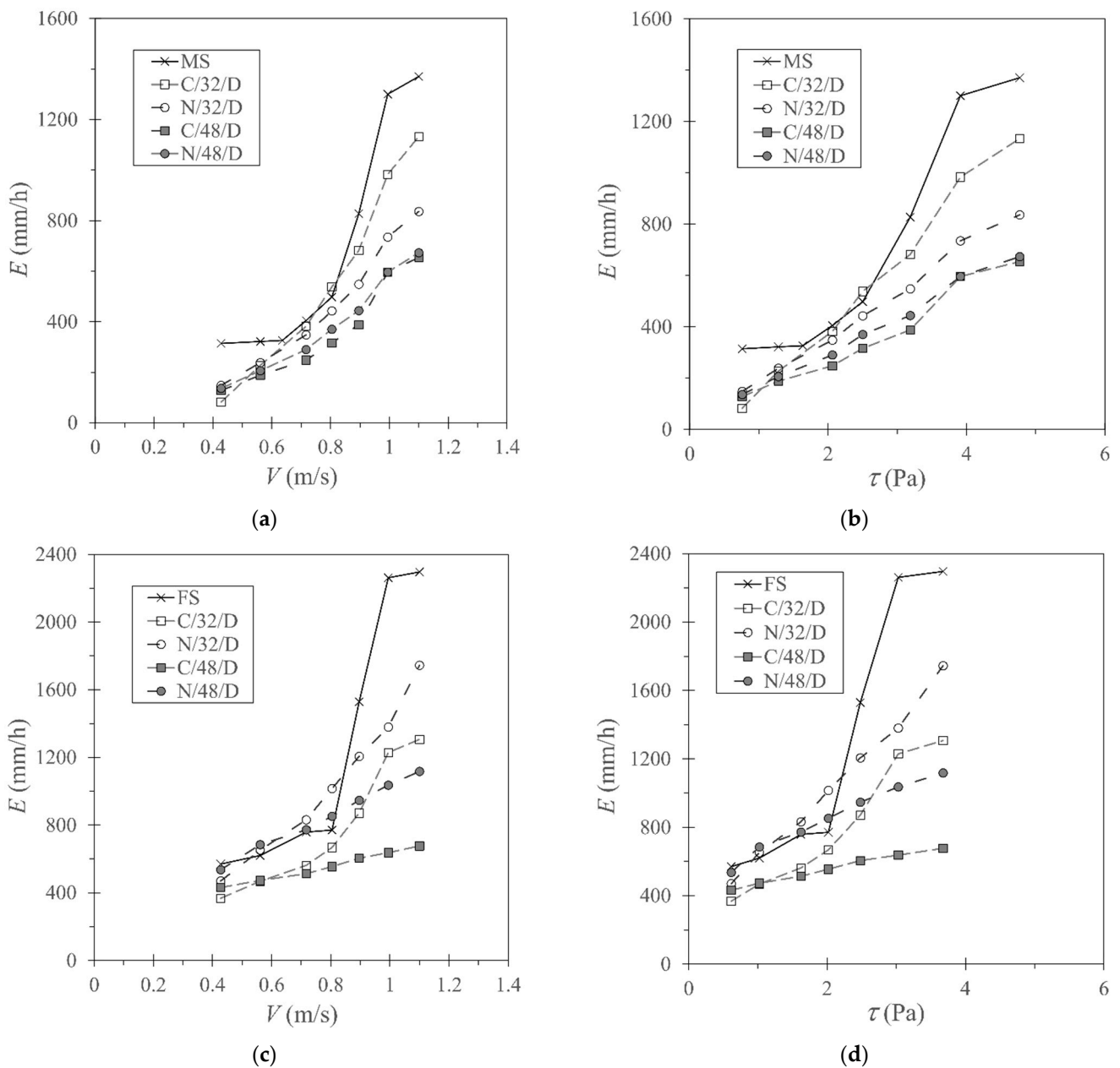


Figure 6. E - V and E - τ erosion-function charts for cyanobacteria-inoculated specimens EFA tested with their BC detached from the container sidewall: (a,b) medium sand; (c,d) fine sand.

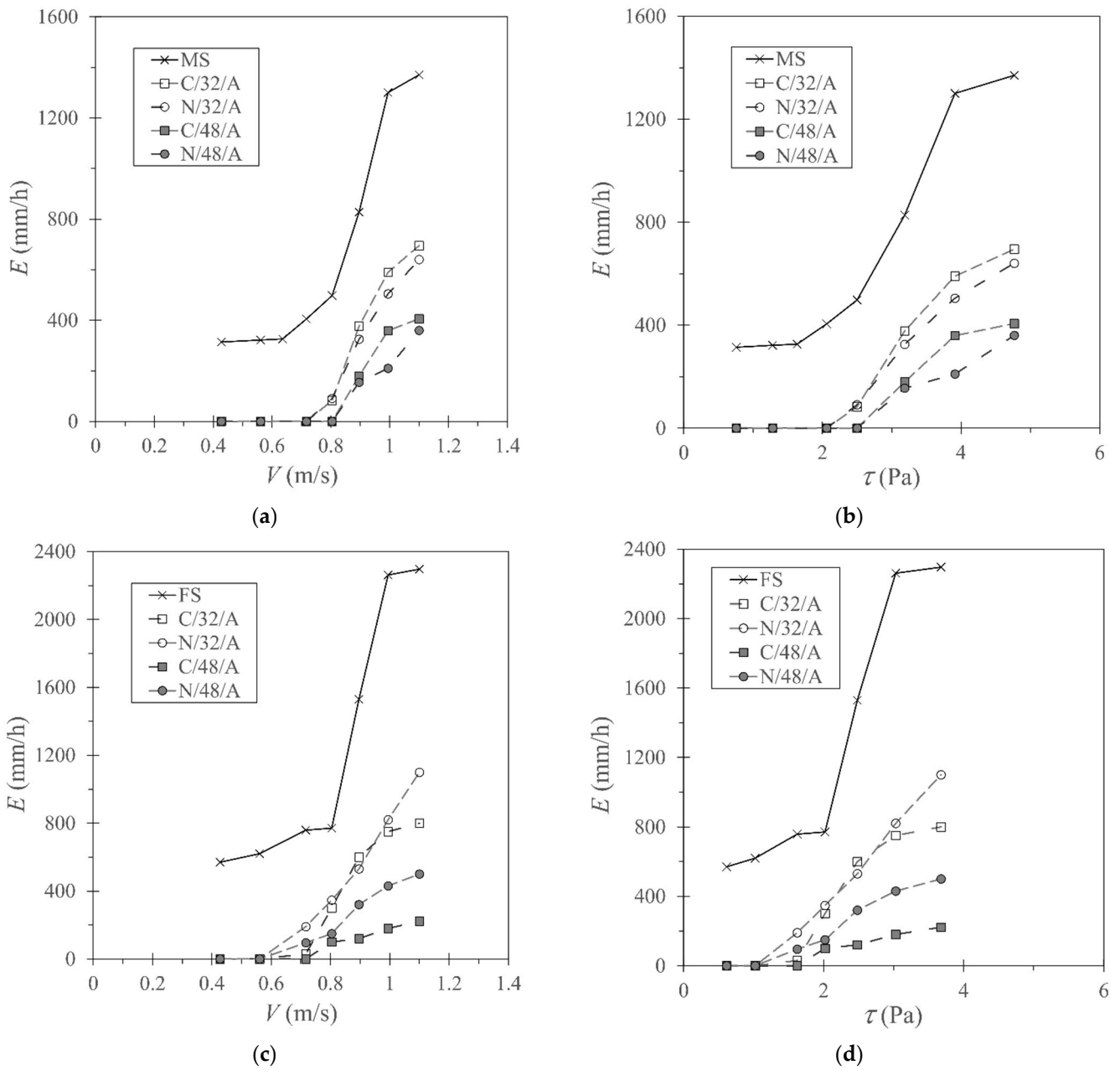


Figure 7. E - V and E - τ erosion-function charts for cyanobacteria-inoculated specimens EFA tested with their BC attached to the container sidewall: (a,b) medium sand; (c,d) fine sand.

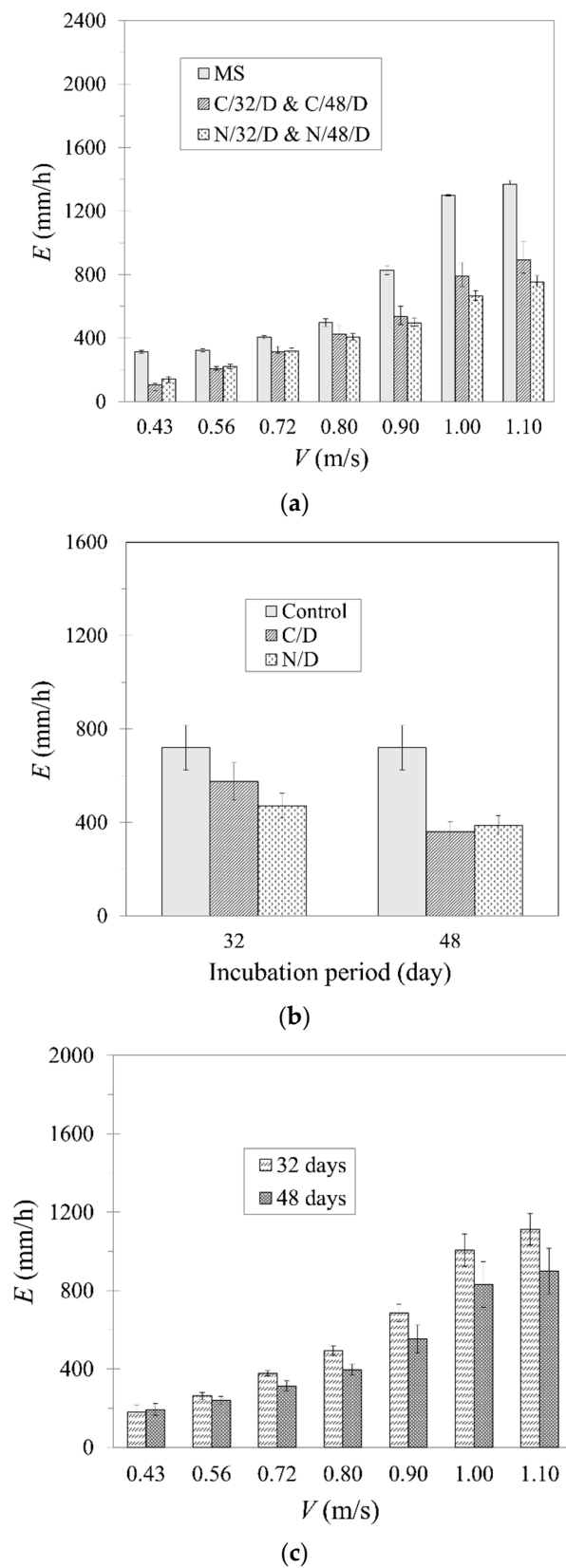


Figure 8. Medium sand specimens EFA tested with detached BC: interdependence of (a) cyanobacterium strain and flow velocity on erosion rate, (b) cyanobacterium strain and incubation period on erosion rate, and (c) incubation period and flow velocity on erosion rate.

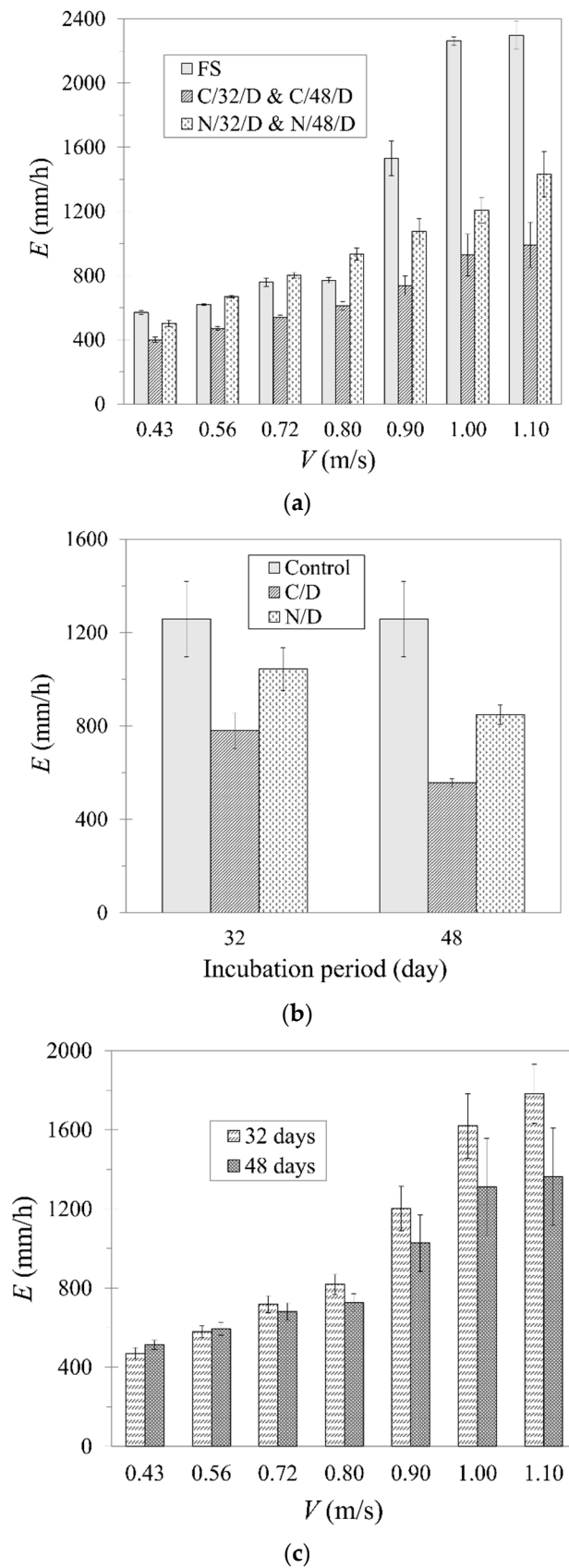


Figure 9. Fine sand specimens EFA tested with detached BC: interdependence of (a) cyanobacterium strain and flow velocity on erosion rate, (b) cyanobacterium strain and incubation period on erosion rate, and (c) incubation period and flow velocity on erosion rate.

4. Analysis of EFA Test Results

Compared to non-inoculated sands, the general trends observable in Figures 6 and 7 are that *Nostoc* and *Calothrix* inoculations, together with longer incubation period (i.e., for 48 days rather than 32 days), have caused significant reductions in the erosion rate, especially for the higher V (τ) magnitude.

For instance, considering the detached BC and comparing with the non-inoculated MS results, the *Nostoc* and *Calothrix* inoculations reduced the erosion rate for 32-day incubated MS by approx. 35% and 20%, respectively, with corresponding values of approx. 46% and 50% for 48-day incubation. Comparing the results for these incubation periods, significant differences between the reductions in erosion rate of the inoculated specimens with detached BC became observable for a flow velocity of greater than 0.72 m/s for the MS and 0.80 m/s for the FS (see Figures 8c and 9c). In the case of the inoculated MS specimens with detached BC, close inspection of Figure 6a,b indicates that for the shorter (32 day) incubation, the *Nostoc* inoculation generally produced marginally better erosion resistance compared to the *Calothrix* inoculation, especially at a higher flow velocity. However, their performances became broadly similar for 48-day incubation (see also Figure 8b). These EFA findings are discussed in Section 5 of this paper in the context of the different cyanobacteria-developed microstructures formed depending on the sand type (gradation) and cyanobacterium strain employed.

In contrast to the above findings for MS, the *Calothrix*-inoculated FS specimens had superior erosion resistance compared to the *Nostoc* inoculation for both 32- and 48-day incubations (Figure 6c,d and Figure 9a,b). For instance, with $V \leq 0.9$ m/s, better overall performance was achieved for *Calothrix* inoculation with 32-day incubation compared to *Nostoc* inoculation with 48-day incubation (Figure 6c,d). Similar overall behaviors were found for FS and MS specimens that had their BC attached to the container sidewall (Figure 7). Overall, compared to non-inoculated FS, the erosion rates for the *Calothrix*- and *Nostoc*- inoculated specimens with attached BC were reduced at 32-day incubation by approx. 38% and 17%, respectively, whereas at 48-day incubation, the respective reductions were 56% and 33%. Again, Section 5 discusses these EFA findings in the context of different cyanobacteria-developed microstructures observed from the SEM examinations.

Values of the erodibility coefficient (K_V and K_τ) and the erodibility threshold (V_c and τ_c) parameters, computed from the erosion-function curves presented in Figures 6 and 7, are listed in Tables 1 and 2 for MS and FS, respectively. Included in these tables are percentage reductions in the erodibility coefficients relative to the non-inoculated group (indicating comparative improvements in soil erosion resistance). Included in Tables 1 and 2 are also the associated erosion categories (ECs), as defined by the classification system based on erodibility thresholds after Briaud et al. [46] (see Table 3). With experimental values of $D_{50} = 0.77$ mm, $V_c = 0.32$ m/s and $\tau_c = 0.49$ Pa for MS, and respective values of 0.23 mm, 0.18 m/s and 0.13 Pa for FS, the non-inoculated materials are described as 'high erodibility' and 'very high erodibility' soils, respectively.

Table 1. Erodibility coefficients and thresholds deduced for medium sand with various cyanobacteria treatments.

	K_V (mm.s/m.h)	$\downarrow K_V$ (%)	K_τ (mm/h.Pa)	$\downarrow K_\tau$ (%)	V_c (m/s)	τ_c (Pa)	Erosion Category
Control	2024	–	323	–	0.32	0.49	2
C/32/D	1596	21.2	269	16.7	0.37	0.59	2
C/48/D	808	60.0	138	57.3	0.37	0.56	2
N/32/D	1048	48.2	177	45.2	0.35	0.50	2
N/48/D	818	59.6	138	57.3	0.37	0.50	2
C/32/A	1138	43.8	199	38.4	0.72	1.80	3
C/48/A	658	67.5	116	64.1	0.80	2.80	3
N/32/A	1017	49.7	178	44.9	0.72	1.90	3
N/48/A	515	74.6	92	71.5	0.80	2.50	3

Note: K_V , K_τ = erodibility coefficients; V_c = threshold flow velocity; and τ_c = critical shear stress.

Table 2. Erodibility coefficients and thresholds deduced for fine sand with various cyanobacteria treatments.

	K_V (mm.s/m.h)	$\downarrow K_V$ (%)	K_τ (mm/h.Pa)	$\downarrow K_\tau$ (%)	V_c (m/s)	τ_c (Pa)	Erosion Category
Control	2901	–	658	–	0.18	0.13	1
C/32/D	1479	49.0	331	49.7	0.22	0.24	2
C/48/D	374	87.1	82	87.6	0.19	0.25	2
N/32/D	1825	37.2	403	38.7	0.22	0.22	2
N/48/D	853	70.6	185	71.8	0.19	0.25	2
C/32/A	1412	51.3	315	52.1	0.69	1.50	3
C/48/A	362	87.5	81	87.6	0.80	2.00	3
N/32/A	1681	42.0	378	42.5	0.60	1.20	3
N/48/A	823	71.6	184	72.0	0.79	1.80	3

Note: K_V , K_τ = erodibility coefficients; V_c = threshold flow velocity; and τ_c = critical shear stress.

Table 3. Erosion category (EC) based on erodibility thresholds (adopted from Briaud et al. [46]).

EC	Erodibility Description	τ_c (Pa)	V_c (m/s)
1	Very high	0.1	0.1
2	High	0.2	0.2
3	Medium	1.3	0.5
4	Low	9.3	1.35
5	Very low	62.0	3.5
6	Non erosive	500	10

Note: V_c = threshold flow velocity; and τ_c = critical shear stress.

5. Discussion and Recommendations for Future Research

The importance of a continuous (undisturbed) BC layer for resisting soil erosion is highlighted by comparing the results presented in Tables 1 and 2 for tested MS and FS specimen groups with attached and detached BCs. In other words, attached BC relates to continuous BC cover over extensive areas of the ground surface, whereas detached BC could be considered analogous to discretized BC cover arising from disturbance in-situ, each separate BC piece approx. 33 cm² (i.e., cross-sectional area of EFA test-specimens). As expected, for all cyanobacteria-inoculation treatments investigated and considering comparable experimental conditions, values of erodibility coefficients for attached BC were lower than those for detached BC, indicating their greater erosion resistance. The extent of the difference in values between them depended on the sand type–cyanobacterium strain combination and specimen incubation period. For instance, considering the *Calothrix*-inoculated MS with 48-day incubation, the K_V value for attached BC was 18.6% lower compared to detached BC [i.e., $(808 - 658) \times 100/808$: refer to Table 1 for these values]. Whereas for FS with the same biological treatment and tested under the same experimental conditions, the K_V value for attached BC was only marginally (i.e., 3.2% [= $(374 - 362) \times 100/374$: refer to Table 2 for these values]) lower compared to detached BC.

Compared to the non-inoculated group, overall erosion rate reductions of approx. one-third and by more than one-half achieved for the cyanobacteria inoculations with 32 and 48-day incubations, respectively, verifies well-developed BCs. SEM examinations demonstrated that different microstructures developed depending on the cyanobacteria strain (*Nostoc* sp. or *Calothrix* sp.) and gradation (i.e., MS or FS) of the loosely deposited sands. For MS, with its larger pore-void spaces, cyanobacteria filaments infiltrated below the specimen surface to significant depth. The lesser infiltration of the *Calothrix* filaments (compared to *Nostoc*) for MS is consistent with the descriptions by [19,48] of the *Calothrix* as a genus with short filaments. Infiltrated filaments of *Nostoc*-excreted dense EPS provided uniform blanket coverage around sand grains and established bridge connections across the wide pore voids, thereby developing a strong aggregation between MS grains and, hence, greater erosion resistance of the MS soil. These features share a number of similarities with observations for other *Nostoc*-inoculated soils [24,28,49]. Whereas the *Calothrix* filaments entangled the sand grains in a net-like structure with low excretion of EPS. Similar observa-

tions to these were reported for different porous environments [23,24,27]. Compared to MS, the low content EPS filaments of *Calothrix* better occupied the FS's smaller pore void spaces, with the observed 3D net-like *Calothrix* structure that entangled the sand grains similar to that observed by [50]. These observations highlight the importance of synergy between the cyanobacterium strain and the nominal pore-void sizes (related to the sand gradation and density state) for achieving improved erosion resistance. The obtained EFA test results were consistent with the above observations. Overall, compared to the *Calothrix* inoculation, the *Nostoc* inoculation achieved, on average, an approx. 1.2-fold greater reduction in erodibility coefficients for MS, with the opposite effect occurring for the cyanobacteria-inoculated FS. Greater erosion resistance for longer incubation (of 48 day) can be explained by the BC developed at 32-day incubation becoming more anchored to the underlying sand layer, because the cyanobacteria filaments had more time to grown and infiltrate deeper into the underlying sand layer's pore voids, especially for the *Nostoc* filaments in MS.

Further laboratory testing and pilot field studies are recommended to corroborate the presented experimental results and to investigate their relation and extension to natural conditions in larger scales. Pertinent questions include whether the cyanobacteria strains can be better applied to the real environment, their overall effectiveness and also the longevity of the applied cyanobacteria. As well as EFA experiments, the laboratory testing could also include, for instance, wind tunnel experiments on larger cyanobacteria-inoculated specimens and BC strength testing using Torvane or pocket penetrometer devices (e.g., see [11]). Field studies are especially necessary to investigate translation and upscaling of the experimental outcomes to practice.

6. Summary and Conclusions

This bench-scale study investigated improvements in the erosion resistance of biologically treated loose silica MS and FS soils (from the drylands of Iran) by inoculating them with single native filamentous cyanobacteria strains (*Nostoc* sp. or *Calothrix* sp). On high exposure to fluorescent light, the cyanobacteria produced well-developed BCs for these low nutrient and highly erodible soils. Within short incubations (of 32 to 48 days), their hydraulic erosion resistance was significantly improved, especially for more severe flow velocities investigated, and highlighted the compatibility of these cyanobacteria strains for treating both sands. These encouraging findings suggest a tailored approach, employing a suitable cyanobacterium strain chosen for its compatibility with the soil's physical properties (i.e., gradation and density state). From an environmental perspective, compelling points of the presented approach are cyanobacteria's resilience to withstand harmful solar radiation and extreme aridness, its ability to self-compensate for disturbance of the BC layer caused by external factors, and its maintenance of the biological diversity of the ecosystem. Unlike some other soil stabilization methods (e.g., MICP), this approach does not involve applying chemical reagents or cause pathogenic behavior to the treated soil. Hence, cyanobacteria inoculation provides the possibility of preserving the life of the natural habitat alongside the land conservation actions. Further laboratory testing and pilot field studies are recommended, especially the field studies to investigate extension of the laboratory results to natural conditions, including practical methods of applying the treatment to very large land areas.

Author Contributions: Conceptualization, A.R. and S.M.A.Z.; methodology, A.R. and S.M.A.Z.; validation, A.R., S.M.A.Z. and B.C.O.; formal analysis, A.R., S.M.A.Z. and B.C.O.; investigation, A.R. and S.M.A.Z.; writing—original draft preparation, A.R. and S.M.A.Z.; writing—review and editing, B.C.O.; visualization, A.R. and B.C.O.; supervision, S.M.A.Z.; funding acquisition, S.M.A.Z. All authors have read and agreed to the published version of the manuscript.

Funding: This research received no external funding.

Data Availability Statement: The original experimental data presented in the paper is available from the corresponding author subject to reasonable request.

Conflicts of Interest: The authors declare no conflict of interest.

Abbreviations

BC	bio-crust
EC	erosion category
EFA	erosion function apparatus
EPS	exopolysaccharide
FS	fine sand
MS	medium sand
SEM	scanning electron microscope
SP	poorly graded
USCS	Unified Soil Classification System

Notations

A_s	specimen cross-sectional area
d_e	mean erosion depth
C_C	coefficient of curvature
C_U	coefficient of uniformity
D	hydraulic diameter (of EFA conduit)
D_{10}	effective grain size
D_{30}	particle size corresponding to 30 wt% passing
D_{50}	mean particle size
D_{60}	particle size corresponding to 60 wt% passing
E	erosion rate
f	friction factor
K_V	erodibility coefficient obtained from $E-V$ erosion function chart
K_τ	erodibility coefficient obtained from $E-\tau$ erosion function chart
R_e	Reynold's number
V	mean flow velocity
V_c	threshold flow velocity
V_e	eroded sand volume
V_v	volume of pore voids
Δt	time interval (EFA test duration)
ϵ'	relative roughness
ν	kinematic viscosity
ρ_w	density of water
τ	hydraulic shear stress acting at soil–water interface
τ_c	critical shear stress

References

- Maier, S.; Schmidt, T.S.B.; Zheng, L.; Peer, T.; Wagner, V.; Grube, M. Specific enrichment of bacterial communities in lichens forming biological soil crusts. *Biodivers. Conserv.* **2014**, *23*, 1735–1755. [[CrossRef](#)]
- Khalilimoghadam, B.; Jabarifar, M.; Bagheri, M.; Shahbazi, E. Effects of land use change on soil splash erosion in the semi-arid region of Iran. *Geoderma* **2015**, *241–242*, 210–220. [[CrossRef](#)]
- Emadodin, I.; Bork, H.R. Degradation of soils as a result of long-term human-induced transformation of the environment in Iran: An overview. *J. Land Use Sci.* **2012**, *7*, 203–219. [[CrossRef](#)]
- Bahrami, A.; Emadodin, I.; Ranjbar Atashi, M.; Bork, H.R. Land-use change and soil degradation: A case study, North of Iran. *Agric. Biol. J. N. Am.* **2010**, *4*, 600–605.
- Mohammadi, S.; Karimzade, H.R.; Alizadeh, M. Spatial estimation of soil erosion in Iran using RUSLE model. *Iran. J. Ecohydrol.* **2018**, *5*, 551–562. [[CrossRef](#)]
- Mosavi, A.H.; Sajedi-Hosseini, F.; Choubin, B.; Taromideh, F.; Rahi, G.; Dineva, A.A. Susceptibility mapping of soil water erosion using machine learning models. *Water* **2020**, *12*, 1995. [[CrossRef](#)]
- Chen, L.; Xie, Z.; Hu, C.; Li, D.; Wang, G.; Liu, Y. Man-made desert algal crusts as affected by environmental factors in Inner Mongolia, China. *J. Arid. Environ.* **2006**, *67*, 521–527. [[CrossRef](#)]
- Parhizkar, M.; Shabanpour, M.; Lucas-Borja, M.E.; Zema, D.A.; Li, S.; Tanaka, N.; Cerdà, A. Effects of length and application rate of rice straw mulch on surface runoff and soil loss under laboratory simulated rainfall. *Int. J. Sediment Res.* **2021**, *36*, 468–478. [[CrossRef](#)]
- Shahrokhi-Shahraki, R.; Zomorodian, S.M.A.; Niazi, A.; O'Kelly, B.C. Improving sand with microbial-induced carbonate precipitation. *Proc. Inst. Civ. Eng.-Ground Improv.* **2015**, *168*, 217–230. [[CrossRef](#)]

10. Amin, M.; Zomorodian, S.M.A.; O'Kelly, B.C. Reducing the hydraulic erosion of sand using microbial-induced carbonate precipitation. *Proc. Inst. Civ. Eng.-Ground Improv.* **2017**, *170*, 112–122. [[CrossRef](#)]
11. Zomorodian, S.M.A.; Ghaffari, H.; O'Kelly, B.C. Stabilisation of crustal sand layer using biocementation technique for wind erosion control. *Aeolian Res.* **2019**, *40*, 34–41. [[CrossRef](#)]
12. Khatami, H.R.; O'Kelly, B.C. Improving mechanical properties of sand using biopolymers. *J. Geotech. Geoenviron. Eng.* **2013**, *139*, 1402–1406. [[CrossRef](#)]
13. Khatami, H.; O'Kelly, B.C. Using Ground Blast-Furnace Slag Grouts with Biopolymer Additives for Improving Sandy Soils. *Proc. Inst. Civ. Eng.-Ground Improv.* **2022**; in press. [[CrossRef](#)]
14. Sujatha, E.R.; O'Kelly, B.C. Biopolymer based soil treatment for geotechnical engineering applications. In *Handbook of Biopolymers*; Thomas, S., AR, A., Jose Chirayil, C., Thomas, B., Eds.; Springer: Singapore, 2023; 18p. [[CrossRef](#)]
15. Rodríguez-Caballero, E.; Belnap, J.; Büdel, B.; Crutzen, P.J.; Andreae, M.O.; Pöschl, U.; Weber, B. Dryland photoautotrophic soil surface communities endangered by global change. *Nat. Geosci.* **2018**, *11*, 185–189. [[CrossRef](#)]
16. Roncero-Ramos, B.; Muñoz-Martín, M.Á.; Chamizo, S.; Fernández-Valbuena, L.; Mendoza, D.; Perona, E.; Cantón, Y.; Mateo, P. Polyphasic evaluation of key cyanobacteria in biocrusts from the most arid region in Europe. *PeerJ* **2019**, *7*, e6169. [[CrossRef](#)] [[PubMed](#)]
17. Becerra-Absalón, I.; Muñoz-Martín, M.Á.; Montejano, G.; Mateo, P. Differences in the cyanobacterial community composition of biocrusts from the drylands of central Mexico. Are there endemic species? *Front. Microbiol.* **2019**, *10*, 937. [[CrossRef](#)] [[PubMed](#)]
18. Lorentz, J.F.; Calijuri, M.L.; Assemany, P.P.; Alves, W.S.; Pereira, O.G. Microalgal biomass as a biofertilizer for pasture cultivation: Plant productivity and chemical composition. *J. Clean. Prod.* **2020**, *276*, 124130. [[CrossRef](#)]
19. Belnap, J.; Eldridge, D. Disturbance and recovery of biological soil crusts. In *Biological Soil Crusts: Structure, Function, and Management*; Belnap, J., Lange, O.L., Eds.; Springer: Berlin/Heidelberg, Germany, 2001; pp. 363–383. [[CrossRef](#)]
20. Büdel, B.; Dulić, T.; Darienko, T.; Rybalka, N.; Friedl, T. Cyanobacteria and algae of biological soil crusts. In *Biological Soil Crusts: An Organizing Principle in Drylands*; Weber, B., Büdel, B., Belnap, J., Eds.; Springer: Cham, Switzerland, 2016; pp. 55–80. [[CrossRef](#)]
21. Malam Issa, O.; Le Bissonnais, Y.; Défarge, C.; Trichet, J. Role of a cyanobacterial cover on structural stability of sandy soils in the Sahelian part of western Niger. *Geoderma* **2001**, *101*, 15–30. [[CrossRef](#)]
22. Mager, D.M.; Thomas, A.D. Extracellular polysaccharides from cyanobacterial soil crusts: A review of their role in dryland soil processes. *J. Arid. Environ.* **2011**, *75*, 91–97. [[CrossRef](#)]
23. Tiwari, O.N.; Bhunia, B.; Mondal, A.; Gopikrishna, K.; Indrama, T. System metabolic engineering of exopolysaccharide-producing cyanobacteria in soil rehabilitation by inducing the formation of biological soil crusts: A review. *J. Clean. Prod.* **2019**, *211*, 70–82. [[CrossRef](#)]
24. Rabiei, A.; Zomorodian, S.M.A.; O'Kelly, B.C. Reducing hydraulic erosion of surficial sand layer by inoculation of cyanobacteria. *Proc. Inst. Civ. Eng.-Ground Improv.* **2022**, *175*, 209–221. [[CrossRef](#)]
25. Moghtaderi, A.; Taghavi, M.; Rezaei, R. Cyanobacteria in biological soil crust of Chadormalu area, Bafq region in central Iran. *Pak. J. Nutr.* **2009**, *8*, 1083–1092. [[CrossRef](#)]
26. Hu, C.; Zhang, D.; Huang, Z.; Liu, Y. The vertical microdistribution of cyanobacteria and green algae within desert crusts and the development of the algal crusts. *Plant Soil* **2003**, *257*, 97–111. [[CrossRef](#)]
27. Lynch, J.M.; Bragg, E. Microorganisms and soil aggregate stability. In *Advances in Soil Science*; Stewart, B.A., Ed.; Springer: New York, NY, USA, 1985; Volume 2, pp. 133–171. [[CrossRef](#)]
28. Malam Issa, O.; Défarge, C.; Le Bissonnais, Y.; Marin, B.; Duval, O.; Bruand, A.; D'Acqui, L.P.; Nordenberg, S.; Annerman, M. Effects of the inoculation of cyanobacteria on the microstructure and the structural stability of a tropical soil. *Plant Soil* **2007**, *290*, 209–219. [[CrossRef](#)]
29. Campbell, S.E. Soil stabilization by prokaryotic desert crust: Implications for Precambrian land biota. *Orig. Life* **1979**, *9*, 335–348. [[CrossRef](#)] [[PubMed](#)]
30. De Caire, G.Z.; de Cano, M.S.; de Mulé, M.Z.; Palma, R.M.; Colombo, K. Exopolysaccharide of *Nostoc muscorum* (cyanobacteria) in the aggregation of soil particles. *J. Appl. Phycol.* **1997**, *9*, 249–253. [[CrossRef](#)]
31. Belnap, J.; Büdel, B.; Lange, O.L. Biological soil crusts: Characteristics and distribution. In *Biological Soil Crusts: Structure, Function, and Management*; Belnap, J., Lange, O.L., Eds.; Springer: Berlin/Heidelberg, Germany, 2001; pp. 3–30. [[CrossRef](#)]
32. Rossi, F.; Li, H.; Liu, Y.; De Philippis, R. Cyanobacterial inoculation (cyanobacterisation): Perspectives for the development of a standardized multifunctional technology for soil fertilization and desertification reversal. *Earth-Sci. Rev.* **2017**, *171*, 28–43. [[CrossRef](#)]
33. Bailey, D.; Mazurak, A.P.; Rosowski, J.R. Aggregation of soil particles by algae. *J. Phycol.* **1973**, *9*, 99–101. [[CrossRef](#)]
34. Rogers, S.L.; Burns, R.G. Changes in aggregate stability, nutrient status, indigenous microbial populations, and seedling emergence, following inoculation of soil with *Nostoc muscorum*. *Biol. Fertil. Soils* **1994**, *18*, 209–215. [[CrossRef](#)]
35. Kheirfam, H.; Sadeghi, S.H.; Darki, B.Z.; Homaeae, M. Controlling rainfall-induced soil loss from small experimental plots through inoculation of bacteria and cyanobacteria. *Catena* **2017**, *152*, 40–46. [[CrossRef](#)]
36. McKenna Neuman, C.; Maxwell, C.D.; Boulton, J.W. Wind transport of sand surfaces crusted with photoautotrophic microorganisms. *Catena* **1996**, *27*, 229–247. [[CrossRef](#)]
37. McKenna Neuman, C.; Maxwell, C. A wind tunnel study of the resilience of three fungal crusts to particle abrasion during aeolian sediment transport. *Catena* **1999**, *38*, 151–173. [[CrossRef](#)]

38. Sadeghi, S.H.; Kheirfam, H.; Darki, B.Z. Controlling runoff generation and soil loss from field experimental plots through inoculating cyanobacteria. *J. Hydrol.* **2020**, *585*, 124814. [[CrossRef](#)]
39. Chamizo, S.; Mugnai, G.; Rossi, F.; Certini, G.; De Philippis, R. Cyanobacteria inoculation improves soil stability and fertility on different textured soils: Gaining insights for applicability in soil restoration. *Front. Environ. Sci.* **2018**, *6*, 49. [[CrossRef](#)]
40. *ASTM D2487-17*; Standard Practice for Classification of Soils for Engineering Purposes (Unified Soil Classification System). ASTM International: West Conshohocken, PA, USA, 2017.
41. Zomorodian, S.M.A.; Soleymani, A.; O’Kelly, B.C. Briefing: Improving erosion resistance of sand using nano-silica additive. *Proc. Inst. Civ. Eng.-Ground Improv.* **2019**, *172*, 3–11. [[CrossRef](#)]
42. Allen, M.M. Simple conditions for growth of unicellular blue-green algae on plates. *J. Phycol.* **1968**, *4*, 1–4. [[CrossRef](#)]
43. Bullard, J.E.; Ockelford, A.; Strong, C.; Aubault, H. Effects of cyanobacterial soil crusts on surface roughness and splash erosion. *J. Geophys. Res. Biogeosci.* **2018**, *123*, 3697–3712. [[CrossRef](#)]
44. Briaud, J.L.; Ting, F.C.K.; Chen, H.C.; Gudavalli, R.; Kwak, K.; Philogene, B.; Han, S.W.; Perugu, S.; Wei, G.; Nurtjahyo, P.; et al. *SRICOS: Prediction of Scour Rate at Bridge Piers*; Texas Transportation Institute, Texas A&M University: College Station, TX, USA, 1999; Report 2937-1.
45. Moody, L.F. Friction factors for pipe flow. *Trans. ASME* **1944**, *66*, 671–684. [[CrossRef](#)]
46. Briaud, J.L.; Govindasamy, A.V.; Shafii, I. Erosion charts for selected geomaterials. *J. Geotech. Geoenviron. Eng.* **2017**, *143*, 04017072. [[CrossRef](#)]
47. Shafii, I.; Shidlovskaya, A.; Briaud, J.L. Investigation into the effect of enzymes on the erodibility of a low-plasticity silt and a silty sand by EFA testing. *J. Geotech. Geoenviron. Eng.* **2019**, *145*, 04019001. [[CrossRef](#)]
48. Rippka, R.; Castenholz, R.W.; Herdman, M. Phylum BX. Cyanobacteria. In *Bergey’s Manual of Systematic Bacteriology: Volume 1—The Archaea and the Deeply Branching and Phototrophic Bacteria*; Boone, D.R., Castenholz, R.W., Garrity, G.M., Eds.; Springer: New York, NY, USA, 2001; Subsection IV; pp. 562–589.
49. Maqubela, M.P.; Mnkeni, P.N.S.; Malam Issa, O.; Pardo, M.T.; D’Acqui, L.P. *Nostoc* cyanobacterial inoculation in South African agricultural soils enhances soil structure, fertility, and maize growth. *Plant Soil* **2009**, *315*, 79–92. [[CrossRef](#)]
50. Aguilar, A.J.; Huber-Sannwald, E.; Belnap, J.; Smart, D.R.; Moreno, J.T.A. Biological soil crusts exhibit a dynamic response to seasonal rain and release from grazing with implications for soil stability. *J. Arid. Environ.* **2009**, *73*, 1158–1169. [[CrossRef](#)]

Disclaimer/Publisher’s Note: The statements, opinions and data contained in all publications are solely those of the individual author(s) and contributor(s) and not of MDPI and/or the editor(s). MDPI and/or the editor(s) disclaim responsibility for any injury to people or property resulting from any ideas, methods, instructions or products referred to in the content.